IEEE 802.11p Empirical Performance Model from Evaluations on Test Tracks

Sébastien Demmel
CARRS-Q, Queensland University of Technology, Brisbane, Australia

Alain Lambert
Université Paris-Sud, CNRS, Institut d'Electronique Fondamentale, Orsay, France
cor. author, email: alain.lambert@u-psud.fr; tel: +33(0)169154081

Dominique Gruyer
IM-LIVIC, IFSTTAR, Versailles, France

Grégoire S. Larue, and Andry Rakotonirainy
CARRS-Q, Queensland University of Technology, Brisbane, Australia

***Abstract*—IEEE 802.11p is the new standard for inter-vehicular communications (IVC) using the 5.9 GHz frequency band; it is planned to be widely deployed to enable cooperative systems. 802.11p uses and performance have been studied theoretically and in simulations over the past years. Unfortunately, many of these results have not been confirmed by on-tracks experimentation. In this paper, we describe field trials of 802.11p technology with our test vehicles; metrics such as maximum range, latency and frame loss are examined. Then, we propose a detailed modelisation of 802.11p that can be used to accurately simulate its performance within Cooperative Systems (CS) applications.**

***Index Terms*—Wireless networks, IEEE 802.11p, DSRC, performance evaluation, empirical modelling**

I. Introduction

IEEE 802.11p is the leading inter-vehicular communications (IVC) technology that has been pushed forward by the IEEE for short-to-medium range communications (up to one kilometre), for both vehicle-to-vehicle (V2V) and vehicle-to-infrastructure (V2I) communications. It is mostly seen as the backbone of Cooperative Systems (CS) applications. The 802.11p amendment to the well-known 802.11 standard (WiFi) was adopted in 2010 and non-prototype hardware is now getting available on the market. Contrary to WiFi technologies used in households' wireless networks, 802.11p uses the 5.9 GHz frequency band and is aimed at the high mobility inherent to vehicular ad-hoc networks (VANETs). Obviously, developing safety-critical systems put certain requirements on the IVC systems that will support them, as they need to guarantee a certain level of performance.

Over the past few years, the performance of 802.11p has been evaluated both in theoretical and simulated studies. Most previous studies [1, 2, 3, 4, 5] used the ns-2 simulator to evaluate the performance of 802.11p. However, the road environment is very complex, always changing, where IVC's performance metrics are likely to diverge from those studied in theoretical simulations. Multiple effects, ranging from Doppler shift, multipath and shadow fading, to simply changing meteorological conditions, can degrade IVC performance. Thus, it is necessary to complement theoretical simulation with field evaluation of the actual IVC performance.

Field performance evaluation of IVC has been ongoing for several years, with research taking off after 802.11a and b had became available [6, 7]. However, we have found that many of the studies aimed at evaluating IVC performance used older versions of 802.11, typically g or g+. For example, Ammoun and Nashashibi [8] evaluated several performance metrics (range, bitrate, etc.) using g+ IVC devices. While such results are interesting, it is fairly straightforward to argue that 802.11g/g+ is no longer relevant to the ITS world. The change in frequency, from 2.4 to 5.9 GHz, means that the behaviour and performance of the IVC device could be fundamentally different, and possibly more in line with results obtained with the older 802.11a at 5.2 GHz.

Nonetheless, a number of recent studies have specifically focused on 802.11p. Böhm *et al.* [9] studied 802.11p performance in a variety of settings (urban, rural) and road configurations (freeway, straight sections, curves, non-flat sections, etc.); they found that 802.11p was still highly subject to line of sight (LoS) effects and that the direction of movement had a significant impact on range, especially at higher speeds. Guo *et al.* [10] also explored 802.11p performance and demonstrated that it could be used for average throughput applications at ranges close to the theoretical limit, although the authors make no mention of experimental conditions such as traffic, the surroundings' density, etc. Shivaldova *et al.* [11] have tested 802.11p performance for an infrastructure-to-vehicle scenario focusing on freeway tunnels and their surroundings; they also highlighted the impact of LoS on the communication's quality. Earlier, both Cheng *et al.* [12] and Tan *et al.* [13] found that the 5.9 GHz channels saw a significant increase in error rates for large packets

Manuscript received 3 October 2013; accepted 15 December, 2013; revised 15 January 2014

compared to smaller packets.

Unfortunately, we note that latencies have not been investigated in these previous studies, when they are supposed to be a major improvement brought upon by the amendment. Furthermore, the whole set of possible speed classes have not been investigated in [8, 10, 11] (each study focuses on a precise range such as lower speeds or freeway speeds). Experimental conditions are not very well known [10] or controlled, notably for being in open traffic [9, 11]. Although it is advantageous to measure performance in real road conditions, as they have shown to be very variable depending on the experimental environment, it is important to obtain baseline performance details in more controlled environments first.

This paper extends preliminary results that have previously been published in Demmel *et al.* [14]: we propose a detailed post-processing analysis of performance metrics (latency, range and frame loss), for measurements taken in a controlled, representative freeway-like environment, and using the full range of speeds achieved by motor vehicles. Using analysis results, we then propose an empirical model to be used in CS-orientated simulation studies. We do not aim to propose a very accurate physical model of 802.11p, that would describe metrics such as the signal strength. Rather, we use our measurements to model the same performance metrics that we measured on tracks, so that they can be used to study CS-based driving assistance applications in simulation environments such as SiVIC [15, 16]. This approach allows us to create a basic but realistic model that requires a low computing power, yet representative enough of actual data. Our proposed model accounts for some interferences and can generate different *frame loss profiles*. A profile represents a single uninterrupted connection between two IVC devices, as long as they are within range. We used profiles in order to cover the large performance variations that we measured, which are influenced by factors such as weather and imperfections in the antennas.

The remainder of this paper is organised as follows: Section II presents the system's architecture used for our measurements (II-A) and introduces the experimental protocol (II-B); Section III offers a detailed performance analysis; Section IV exhibits our modelisation of 802.11p performance; eventually, we offer conclusions and perspective on future works in Section V.

II. Experimental Set-up

A. System Architecture

We performed our field measurements on 2 instrumented vehicles: a Renault Clio 3 and a Citroën C4 Grand Picasso. The vehicles are fitted with powered equipment racks in the boot and several in-cabin screens for HMI. A variety of sensors can be fitted on them depending on the experimental requirements. Our experimental architecture features an IVC device, a host computer, a RTK GPS device and a NTP time server; all are duplicated in each vehicle (see Fig. 1).

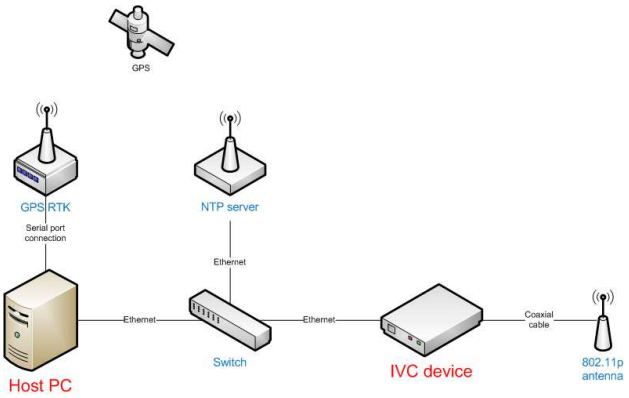

Figure 1: Hardware architecture used for the measurements

The IVC device are independent computer boards fitted with Atheros 5413 WiFi chipsets, the same that we used in the CVIS project [17]. We installed the open-source ath5k WiFi driver, which was patched in 2010 for the Grand Cooperative Driving Challenge (by team "*Scoop*", see Mårtensson *et al.* [18]) in order to enable 802.11p channels. Ad-hoc mode and IPv4 are used; note that the *dot11OCBEnabled* flag is set to *false*, so that normal 802.11 ad-hoc behaviour is used. Although this option was designed to reduce latency for high-priority safety-related frames, all 802.11p frames need not to use it. Furthermore, it is interesting to evaluate 802.11p latency in a more "classical" 802.11 architecture, so that, with further work, the actual interest of the *dot11OCBEnabled* flag can be assessed. The IVC device is connected to a roof-mounted 8 dBi gain stick antenna. The chipset's transmission power is lowered to 20 dBm, so that, accounting for all connectors and cable attenuation (estimated at 2.5 dBm from manufacturer's data), the effective isotropically radiated power (EIRP) is $20-2.5+8=25.5$ dBm, or 355 mW. This value was chosen in order to: (1) remain under regulation for the concerned frequency band; and (2) allow signal's natural extinction within line of sight and within 802.11p's theoretical range (1,000 metres, according to official specifications [19]). The maximum EIRP in the 802.11p band (5.875-5.905 GHz), as regulated by the ARCEP (France's Telecommunications and Posts Regulation Agency), is 33 dBm, approximately 2 Watts. It is in line with the European Commission's harmonisation regulation for ITS usage of the 5.9 GHz band (see Fig. 2, for the European and American regulations; the European regulations incorporate two channels that are reserved for future use, shown in grey). We operated on the 5.890 GHz channel, which is the dedicated control channel according to the American spectrum allocation, but has no specific allocation in the European scheme.

A custom Java application hosted on the IVC device was the principle method used to collect data. It sends a UDP frame through a Java datagram socket to the IP address of the target vehicle, at a frequency set by the user; by default, a deterministic timer is used to generate

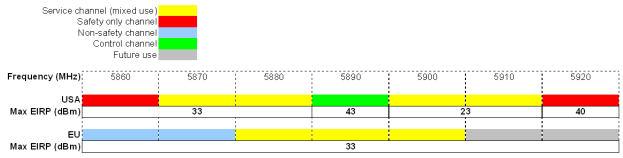

Figure 2: Spectrum allocations and EIRP limits in the USA and EU

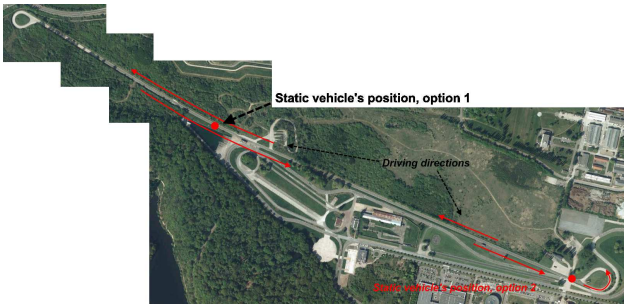

Figure 3: Map of the arrangements for the measurements on Satory's tracks

frames at 20 Hz. A typical frame's payload size is 20 bytes. The actual frame at the MAC level also includes: 8 bytes of UDP header, 20 bytes of IP header, 8 bytes for LLC, and 28 additional bytes of overheads including the 802.11 MAC preamble and header, as well as the CRC sequence. This adds to a total of 84 bytes.

As our research focus is mostly on Emergency Electronic Brake Light (EEBL) [20] applications (see also [21, 22]), we chose to use a frame size in line with EEBL's requirements. In ref. [23], the recommended payload for EEBL frames is 36 bytes, and includes detailed information on the emitter's behaviour. Some data fields listed in the cited report, such as the vehicle's size and the GPS antenna's offset can probably be removed without affecting the application's usefulness. Thus, we believe that 20 bytes is a good compromise for an EEBL frame that can include a vehicle's ID, location, and timing information. The application computes the latency based on the frame's emission time recorded in it. A log file is automatically generated containing the frame's information: computed latency, payload size, received power (signal strength indicator) and reception time. Frame loss and bitrate can be processed from this log file. The 802.11p and frame parameters are summarised in Table I.

A RTK GPS device records positioning data at a 5 Hz frequency on the host computer. Time synchronisation, which is critical for any safety application and for accurately measuring latencies, is performed with Brandywine Network Time Adapters (BNTA), one per vehicle, which distribute accurate timing information from GPS through a NTP architecture (the BNTA's clocks are specified to remain within 25 nanoseconds of the GPS reference). Within the NTP architecture, the BNTA is a *stratum* 1 time server, as it is directly referenced to GPS satellite-based clocks (*stratum* 0). As such, the IVC device and host computer are clients of *stratum* 2. The BTNA is set in

Table I: 802.11p and frames parameters

Parameter	Value
Frequency	5.890 GHz
TX power (at chipset)	20 dBm
Antenna type, gain	Omnidirectional, 8 dBi
EIRP	~25.5 dBm (355 mW)
Frame size	64 (headers) + 20 (payload) bytes
Frame frequency	20 Hz

broadcast mode, sending timing information to its clients four times a second. The drift between the GPS reference time and our devices' clocks (and in consequence between the devices themselves) was experimentally verified to be less than 1 millisecond.

B. Experimental Protocol

The principal experimental protocol is kept voluntarily simple. The scenario has a receptor vehicle (usually the Citroën C4) passing by a static emitter (usually the Renault Clio), which is located on the track's side. We consider V2V and V2I communications to be equivalent for our measurements. Indeed, it is suggested by previous research [8, 9], and LIVIC's experience, that the absolute speed of 802.11 emitters and receptors in the environment's referential does not have much effects on IVC's quality. On the other hand, the speed difference between the emitter and the receptor is a major parameter. As we consider a static emitter, the speed difference and speed relative to the environment are equivalent. The following speeds were tested: 30, 50, 70, 130 and 170 km/h (approximately 20, 30, 45, 80 and 105 mph). Data originally collected using this protocol shall be known as the *2011 dataset*.

A similar protocol was used for additional measurements (henceforth, the *2012 dataset*) aimed at measuring non-omnidirectionalities in the antennas and the influence of the vehicle's body shape on received signal strength. More specific details on the modifications between the 2011 and 2012 experimental protocol will be given in Section III, whenever necessary.

Measurements were performed on Satory's test tracks, isolated from regular traffic. The principal test location was the speed track, a 2-kilometres-long quasi-straight line, with 2 lanes, allowing for 1.4 kilometres of direct line of sight (LoS). The emitter was either located at the track's eastern end, or near a slight bend, so to have LoS with all the track's length (see map in Fig. 3). The track's surroundings are largely open, despite a few sections with overreaching trees. Additional measurements were performed on other tracks of the Satory's site, such as *la routière* track, equivalent to a French non-segregated trunk road (*route nationale*). Measurements location will be mentioned in the performance analysis, if necessary.

Overall, data were collected on 10 different days spread out from September to December 2011 (*2011 dataset*) and from January to February 2012 (*2012 dataset*), with a total of over 400 kilometres driven during experiments. Meteorological conditions were quite variable from day

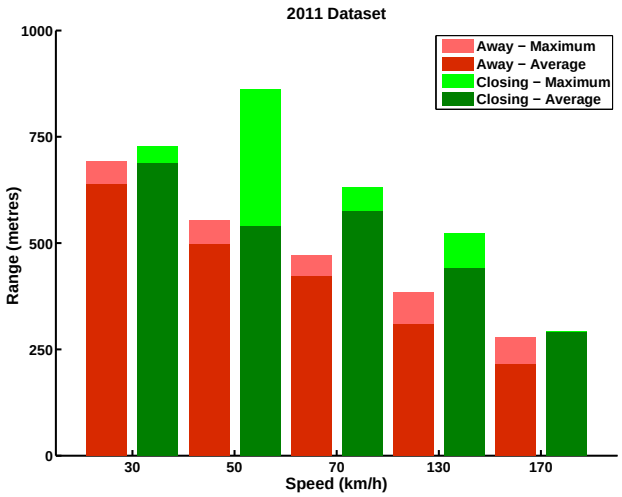

Figure 4: Analysis of maximum transmission ranges obtained during our data collection

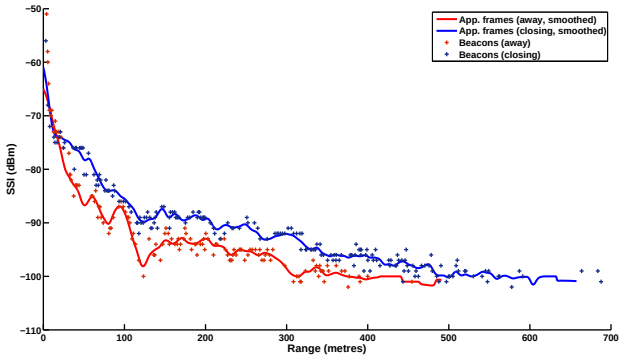

Figure 5: SSI according to direction of driving, for beacons and application frames (single drive pictured)

to day; most measurements took place on typical Parisian winter overcast days, but we also gathered data during dry, sunny conditions or light rain.

For the remainder of this paper: "*closing*" will refer to items relevant to when the receptor vehicle is moving toward the emitter; "*away*" will refer to items relevant to when the receptor vehicle is moving away from the emitter.

III. Performance Analysis

A. Range

The range is the maximum distance at which a frame is successfully received by the receptor vehicle from the emitter (when frame loss is almost 100%); thus what we call the range is actually the *transmission range*. The physical carrier sensing range is not taken into account in this study. The range is estimated based on the receptor's localisation process that uses RTK GPS data.

Fig. 4 is a plot of all the average and maximum ranges, classified according to speed (from 30 to 170 km/h) and direction of driving (*2011 dataset*). The average standard deviations is approximatively 16% of the average range. Data show a clear inverse relationship between relative

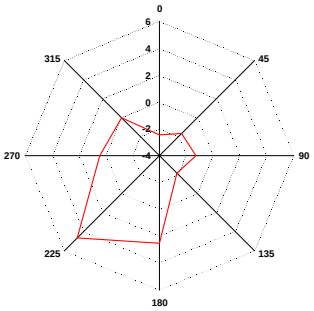

Figure 6: Differences with the average SSI (in dBm) for 8 angular sectors (in degrees) of the receiving antenna

speed and range. Doppler effects likely explain the range reduction with increased speeds, which was verified for the whole data. Maximum measured ranges are relatively consistent, with only the "50 km/h - closing" setting showing a larger variability (it also had the largest measured range in the *2011 dataset*), which can be explained by changing environmental conditions over several days of measurements.

One can note significant differences between the closing and away ranges at the same speeds, with the closing range being greater than away range. This relates to findings in Böhm *et al.* [9] (and [8] in 802.11g); however, their data are reversed compared to ours: away range is greater than closing range. We shall investigate the effect explaining the original dataset's behaviour in the remainder of this subsection.

Setting up a virtual interface working in monitor mode allowed to access management frames and beacons while our measurement application was running. We thus performed additional measurements in the exact same experimental conditions as previously, in order to determine whether the user transmission on the IP stack had any effect on the results. Our investigation suggests that there is no significant difference between the range for management frames (beacons included) and for applications' frames in the speed track setting. However, the direction of driving produces the same influence over the maximum range of beacons and applications' frames, which suggests that this difference is due to an actual physical effect.

Consequently, we have investigated the Signal Strength Indicator (SSI) for various speeds. Fig. 5 shows the recorded SSI for a typical drive at 70 km/h, in both directions, extracted from the *2011 dataset*. One can clearly see that two "paths" exists: the SSI is consistently lower when the vehicle drives away, compared to when the vehicle drives toward the emitter. Note that the chipset's reception threshold is -101 dBm; this threshold governs whether frames can still be exchanged between the emitter and the receptor, thus crossing it defines the maximum range. Two factors could explain this measured SSI difference: (1) an imperfect omnidirectionality of the antennas (in the horizontal plane), and (2) an influence of the vehicle's body. Indeed, during the *2011 dataset*'s collection, the orientation of the antennas and vehicles on the track

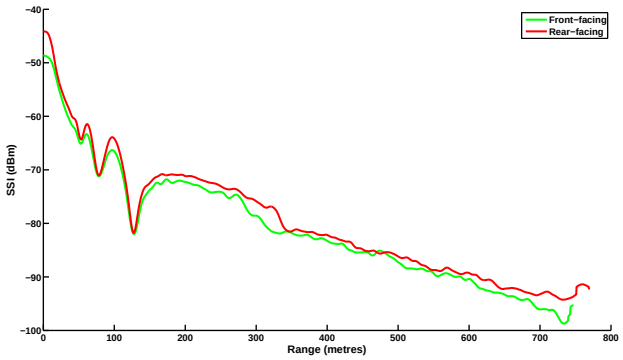

Figure 7: Smoothed (Nadaraya-Watson kernel regression) SSI measured at 50 km/h (for a single drive), alternating the side of the vehicle facing the emitter (antenna's orientation is always maintained), from the *2012 dataset*

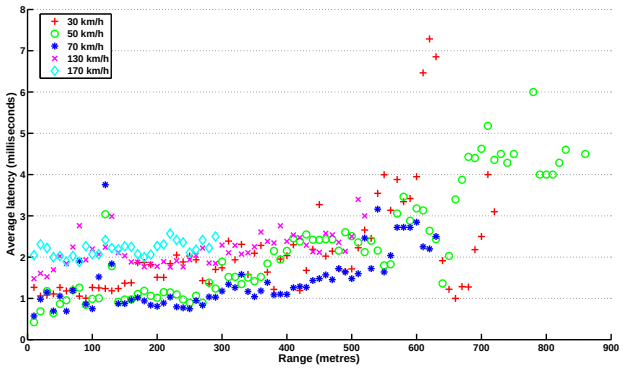

Figure 8: Average latencies for all speeds, according to range

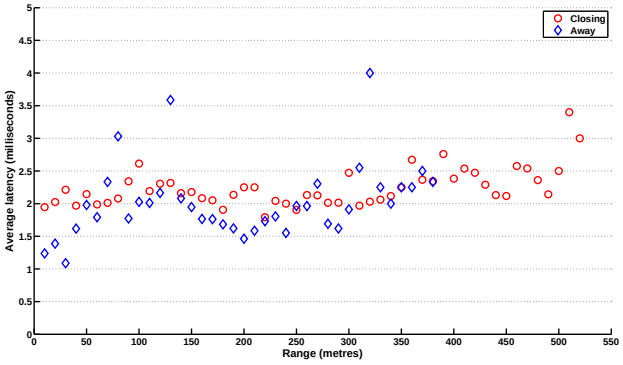

Figure 9: Influence of the direction of movement on latency, measured averages for 130 km/h

(hence which sides faced each other) was not controlled.

For the first factor (omnidirectionality), we focused on the receptor's antenna, as we assumed it was the one that would be affecting the most received power during a normal experimental drive. We measured the SSI for 8 orientations of the antenna, rotated 45 degrees from each previous time (the initial orientation, angle 0, was chosen arbitrarily); the emitting antenna remained completely static meanwhile, and the vehicle's relative orientation did not change. Fig. 6 shows the averaged differences between the overall average SSI and the measured SSI for each angle, demonstrating that the antenna is not perfectly omnidirectional. For example the difference between the 45-225 degrees axis is at least 6 dBm. This would be sufficient to explain the large range difference between closing and away conditions we found in our initial measurements. Indeed, the difference measured on the signal shown on Fig. 5 averages to 5 dBm.

For the second factor (vehicle's body), we measured how the SSI behaves when the receptor vehicle is moving either away from the emitter or closing to it, alternatively front and rear-facing, at a fixed speed (50 km/h). The antennas' relative orientation was maintained throughout the whole measurement session, so that the non-omnidirectionality did not affect the experiment. Our measurements show that the vehicle's orientation (and thus shape) has an influence on the received power of no more than 2 dBm (see Fig. 7).

We performed a third experiment measuring SSI in order to determine whether the direction of driving had a real influence on the range, and, if yes, what was its strength. The vehicle is moving away from and back to the emitter, but always facing the same direction, controlling for its shape and the antennas' relative orientation. The measured difference was not significant compared to the other factors like the vehicle's body or the antenna's non-omnidirectionality.

Böhm *et al.* [9] claim that they measured a difference due to the direction of travel even at walking speed, which allows them to rule out Doppler effects as a possible source for their range difference. Measurements obtained with our set-up at low speeds (<10 km/h) do not show any significant difference between each direction of driving. It is probable that their finding can be attributed to non perfectly omnidirectional antennas. Similarly, the range difference related to the direction of driving that they found, at normal driving speeds, can also probably be explained by non-omnidirectionality. Ammoun and Nashashibi [8] also measured this difference in 802.11g and attributed it to signal validation mechanisms using different power thresholds for the establishment or the loss of a connection. However, they performed their measurements in Infrastructure mode, while both Böhm *et al.* [9] and ourselves worked in Ad-hoc mode. It is probable that non-omnidirectionality also significantly affected their results.

The largest range for all measurements is 1,397 metres. Nonetheless, most of the measured maximum ranges were largely under specifications or ranges measured in other studies. As specified in Section II-A, the transmission power was lowered to remain in line with 802.11p specifications. In Böhm *et al.* [9], the transmission power was actually slightly lower than ours (17 versus 20dBm, at the chipset), yet they achieved larger ranges; it is probable that they had lower attenuation in their cables and connectors. Informal measurements with $Tx\,power = 33\,dBm$ suggested no difficulty in achieving kilometric range systematically with larger powers.

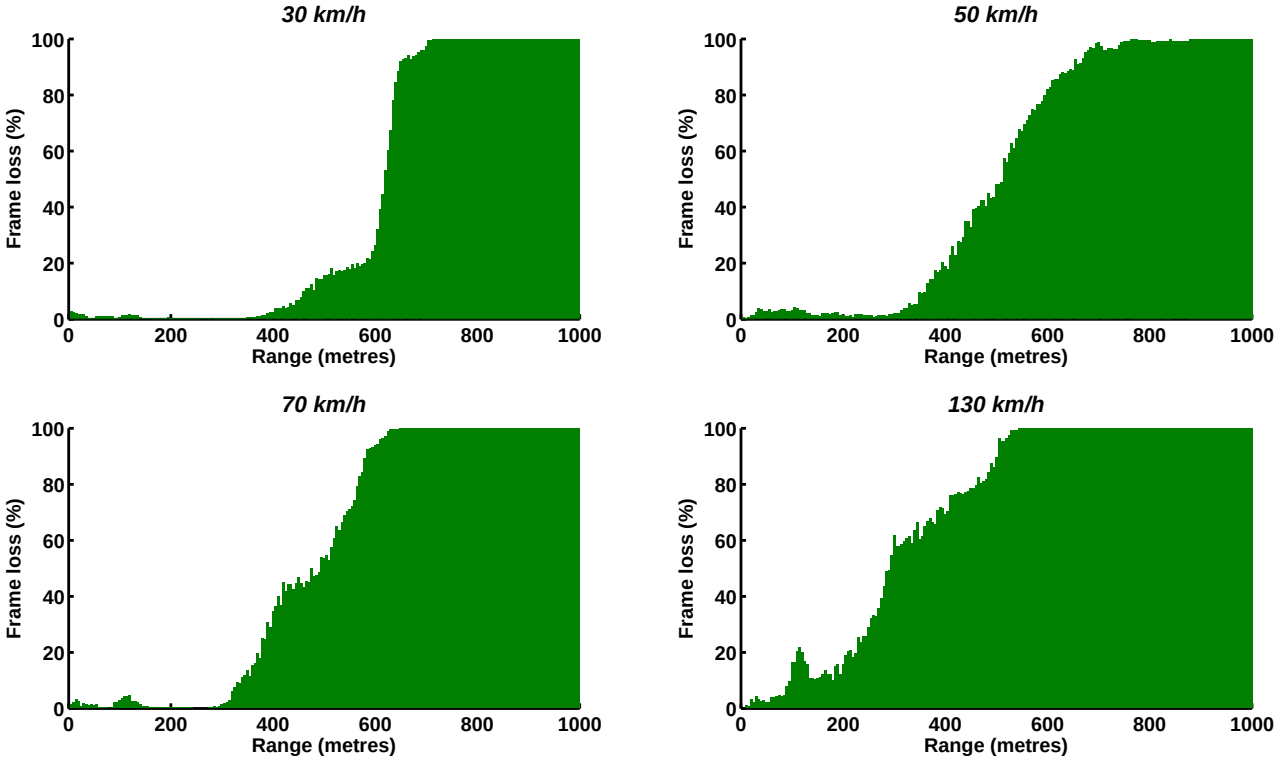

Figure 10: Detailed average frame loss measurements for 30, 50, 70, and 130 km/h

B. Latency

We define latency as the temporal delay between the generation of a frame at the emitting device, and its reception at the receptor device. More precisely, we consider the time when the message is generated and sent to the transport layer (UDP) through the socket; similarly, the reception time is set at the instant the frame is read by the application in the receptor vehicle. Thus, latency includes IP, MAC, and physical layers latencies. We have not tried to measure the specific latencies at each layer, as our main interest resides in the application-to-application latency. Indeed, knowing the global latency is essential to design robust vehicular safety applications.

Fig. 8 shows the average latencies measured at 30, 50, 70, 130 and 170 km/h. The average latency is centred around 1.5 milliseconds. The direction of movement does not have any influence on the latencies, as illustrated by Fig. 9, showing data for 130 km/h. In this example, latency is stable within the "useful" range, until 400 metres (where frame loss remains under 50%), and is similar for both direction of movement. For ranges greater than 400 metres, averages are based on fewer measurement points as the number of lost frames increase considerably (see Section III-C for a detailed analysis of frame loss). It is probable that latency is sometimes increased at these large ranges when the underlying management processes in 802.11 introduce latencies as they struggle to maintain IBSS (Independent Basic Service Set) membership over a degraded medium link (especially considering we did not use the *dot11OCBEnabled* option). Indeed, a number of beacons and other management frames have to be exchanged before any useful transmission can take place. At long ranges, IBSS membership can be lost and regained several times, as even management frames have difficulties getting properly transmitted. An application frame can thus be stored in a buffer for a a few milliseconds before communication is again possible within the IBSS group.

We can conclude that, according to our results, average latencies are not dependent on the vehicles' relative speed, either on the transmission range, at least not until extreme ranges where frames starts to get missed. Overall, latencies remained inferior to 5 milliseconds 99.47% of the time.

C. Frame Loss

The last indicator we investigated is frame loss. Frame loss is defined as the percentage of frames that are missed during a certain measurement interval. It is straightforward to deduce the actual bitrate from the nominal bitrate and the measured frame loss. The maximum range is an important indicator, but does not say anything about the quality of transmissions *within* this range. Typically, one could receive frames up to a thousand metres, yet have 80% frame loss starting as soon as 500 metres away from the emitter. Thus, it is also important to measure the quality of transmission within the transmission range, typically via frame loss.

Fig. 10 presents the average frame loss measured over the whole range, at 5 metres intervals. One can note slight fluctuations within the transmission range, at all speeds. Some of these can be explained by environmental

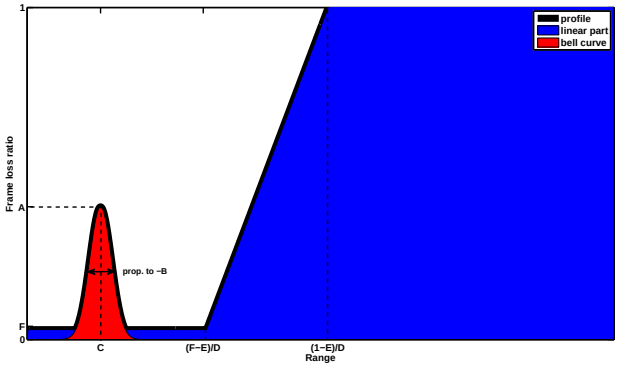

Figure 11: Decomposition of a frame loss profile τ, with its parameters

features that degrade the transmission's quality (scattering leading to multipath, interferences, degraded LoS, etc.). A typical example are the destructive interferences that build up because of signal reflected from the ground (Two-Rays propagation model), which can be seen on most sub-graphs at distances of 100-150 metres (especially at 130 km/h). Because of these interferences, the SSI drops closer to, or under, the chipset's reception threshold, which explains why frames are missed. Changing meteorological conditions affected the signal's quality too, even if we have not controlled for them. Broadly, the frame loss is also an inverted metric of the percentage of frames which are above the chipset's reception threshold.

IV. 802.11p Frame Loss Model

A. Rationale

As we mentioned in the introduction, many simulation studies of 802.11p usage have been using ns-X family simulators. In section III, we have shown that the road environment complexity means that, in most cases, 802.11p performance metrics are likely to diverge considerably from expected theoretical models. NS-family simulator can be configured to use a Two-Ray Ground propagation model. Our experimental data suggest that this model is not capable of representing all the performance variations that we measured.

Empirical modelisation is a good avenue to improve simulations' results. Recent developments have shown interesting approaches, such as using a Two-Ray Interference model for LoS conditions [24], or improving non-LoS conditions [25, 26]. Nevertheless, the aforementioned papers have in common to focus on the actual signal propagation rather than modelling important performance metrics of 802.11p (range and frame loss). Such a modelling would enable us to support higher-level simulations of CS applications performance directly.

Range can be understood as a subset of frame loss: indeed, the maximum range simply express the distance at which frame loss is always 100%. We thus focus only on modelling frame loss from our experimental data. Overall, the model's inputs are the distance and relative speed between two communicating devices (vehicles or roadside device); the model's output is a frame loss probability for the given inputs. We chose straightforward mathematical functions that are able to reproduce experimental data, present some variability, and that can also be easily adapted to new datasets when additional data become available.

Additionally, the model will be able to reproduce the experimental data but will also allow generating "new" data, i.e. runs that have not been measured but that are plausible, given the measurements. Because of the environments where the measurements campaign took place, our model will be appropriate for open freeway-type environments, as well as rural roads and possibly low-density suburban ones. We do not claim that our model works for urban situations, or for non-LoS conditions.

At first, in subsection IV-B we will detail the model's mathematical foundation and its relationship to measurements. Then, in subsection IV-C, experimental data are broken down in a number of classes before the model's parameters are estimated. Eventually, in subsection IV-D, we explain how profiles can be generated during a simulation.

B. Individual Frame Loss Profiles

We use a new approach that we named *frame loss profiles*. A profile represents a single uninterrupted connection between two IVC devices and is used to determine the frame loss probability at any given distance, as long as they are within range (that is, as long as frame loss is under 100%). By generating different profiles we can thus cover the large variations we measured, which are influenced by factors such as weather and imperfections in the antennas. This approach also allows to have a temporally consistent frame loss probability and to avoid unrealistic probability shifts at two consecutive distances that could arise from using a simple "average-plus-noise" model of the whole measurements. A single frame loss profile τ is described by:

$$\begin{aligned} \tau &= \max\left[A.\exp^{B.(d-C)^2}; \ldots\right. \\ &\ldots \quad \left.\min\left(\max\left[D.d+E;F\right];1\right)\right] \end{aligned} \tag{1}$$

where d is the distance between the emitter and receptor; and $A, B, \ldots F$ are parameters estimated from empirical data. Broadly, τ is the addition of several models, as illustrated on Fig. 11.

Term $A.\exp^{B.(d-C)^2}$ represents the frame loss area corresponding to the strongest ground reflection interferences, centred at distance C. At this point the ground-reflected signal is strong enough to cancel out a large proportion of the incoming direct signal's energy, pushing a proportion of frames under the chipset reception's threshold; the frame loss corresponding to this proportion is represented by A. The bell curve's width is proportional to B; note that B is always negative. The model assumes that no counter-measure is applied to reduce the frame loss induced by interferences at C.

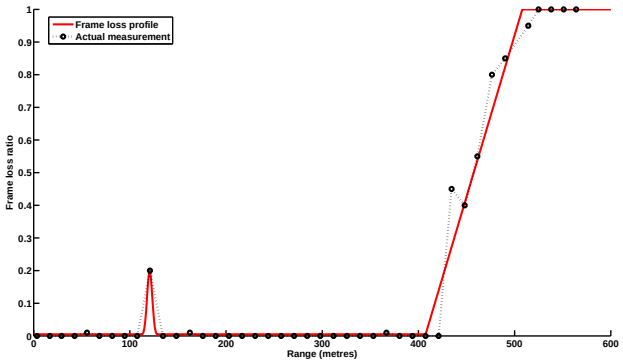

Figure 12: Comparison of a frame loss profile versus the corresponding actual measurement

Term $D.d+E$ is a linear regression where τ is modelled linearly as a function of distance d and parameters D and E. This term represents the progressive increase of frame loss as received signal strength decrease. The increase starts from a non-zero frame loss ratio value given by parameter F, which represent the average of small perturbations measured within range. Typically, F will be low (less than 5%). D and E have two meaningful ratios: ratio $\frac{F-E}{D}$ gives the distance at which frame loss starts to increase from the plateau at F; ratio $\frac{1-E}{D}$ expresses the distance at which frame loss reaches 100%, hence the maximum range.

By using profiles, we focus on modelling individual measurement runs rather than the average frame loss as shown for all runs on Fig. 10. For each individual measurement, the model's parameters $A,B,\ldots F$ are estimated using the Levenberg-Marquardt algorithm for non-linear least squares [27]. An instance of an obtained profile compared to a typical individual measurement run is shown on Fig. 12.

C. Frame Loss Profiles Classes

We created four classes of individual frame loss profiles, which are classified according to the relative speed between the emitter and receptor:

$$speed = [0;40],[40;60],[60;100],[100;160]$$

For each class, the experimental data show that D and E are linearly correlated. The other parameters are assumed to be independent. The relationship between D and E is given by a Generalised Linear Model regression from the observed values of D and E:

$$E = \alpha D + \beta + e \quad e \rightsquigarrow \mathscr{N}(0,\sigma) \tag{2}$$

For each class and each parameter A,B,C,D,F (excluding E), a non-parametric probability density estimate is computed: the continuous distribution $\mathbf{A},\mathbf{B},\mathbf{C},\mathbf{D},\mathbf{F}$ of each parameter A,B,C,D,F is computed with a Gaussian kernel smoothing method (the distribution $\mathbf{E}$ of the parameter E can be obtained through its linear correlation with $\mathbf{D}$).

D. Profiles Generation

In a simulation environment such as presented Gruyer *et al.* [16], the parameters' distributions are used to generate realistic random parameters for the frame loss profile model. To generate sets of parameters, the inverse transform sampling method is used. The $\mathbf{A},\mathbf{B},\mathbf{C},\mathbf{D},\mathbf{F}$ distributions for each class are transformed into cumulative distribution functions $G_{\mathbf{x}}$ where $\mathbf{x} \in \{\mathbf{A},\mathbf{B},\mathbf{C},\mathbf{D},\mathbf{F}\}$. These cumulative distributions are then used as follows:

1) For each $x \in \{A,B,C,D,F\}$ // x is a parameter and $\mathbf{x}$ its distribution
   a) $u \leftarrow \mathscr{U}(0,1)$ // a random number u is generated from the uniform distribution $\mathscr{U}(0,1)$
   b) $x \leftarrow G_{\mathbf{x}}^{-1}(u)$ // a parameter receives the value from its inverse cumulative distribution
2) End For
3) $E \leftarrow \alpha D+\beta+e$ // E is obtained from the linear relationship that links it to D, where α and β are the regression parameters and e is the Gaussian noise $e \rightsquigarrow \mathscr{N}(0,\sigma)$
4) $\tau = \max\left[A.\exp^{B.(d-C)^2};\min\left(\max\left[D.d+E;F\right];1\right)\right]$ // Once each parameter has been assigned a value, τ can be processed from the values with Eq. (1)

Fig. 13a shows the range that our model can achieve in generating individual frame loss profiles (in the $[60;100]$ class); each curve is a single different set of drawings of u for the parameters. The ground-reflection interference remain concentrated around the 120 metres mark (as shown in the zoomed-in graph from Fig. 13b), and the rising part shows a large range of variability: the best case profile allowed an error-free connection between two nodes until almost 700 metres, while on the other hand the worst case profile returned to a low loss probability for only a short distance after passing the ground interference area, yielding a total range of barely 250 metres. In this example, the model's parameters so that they can generate profiles over a larger range than measured on tracks. However, by computing the average of many generated profiles we obtain curves that reproduce closely the average measurements, as shown on Fig. 14 for the averages of a thousand profiles of each class. Each individual profile represent a set of specific conditions that could be found on the road; a profile can represent realistically the conditions on a sunny or on a rainy day. Changing the parameters of the Gaussian kernel smoothing method allows generating distributions for the model's parameters that either closely reproduce experimental data or, on the other hand, that allow non-measured but plausible profiles.

In a simulated environment, a profile can be generated each time a connection is established between 2 nodes (typically when the enter within a static maximum range threshold); one emitter can have several profiles active at the same time if it is connected with more than one receptor.

However, this approach has a few limitations. At first, there is no way to known which conditions resulted in a particular profile. If two neighbouring vehicles are connected to a same emitter, it is possible that one vehicle has a profile corresponding to dry, sunny weather while the other has humid, overcast conditions. Secondly, the

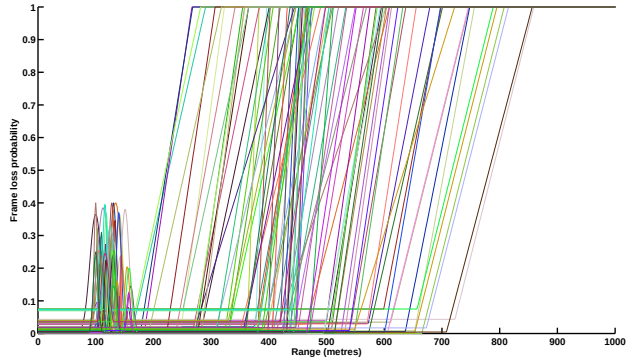

(a) Frame loss profiles generated with 100 sets of drawings of u

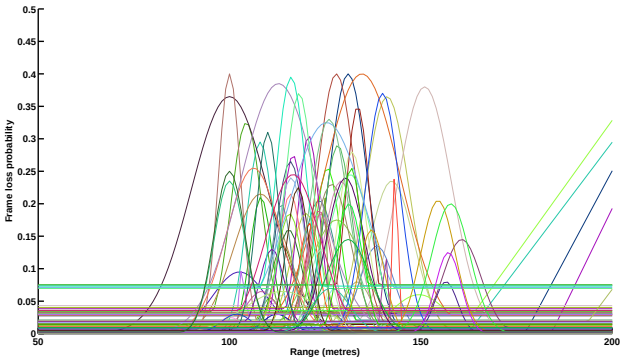

(b) Zoom on the frame loss peaks caused by ground-reflection interferences, for 100 sets of drawings of u

Figure 13: Generation of frame loss profiles for the [60;100] km/h class

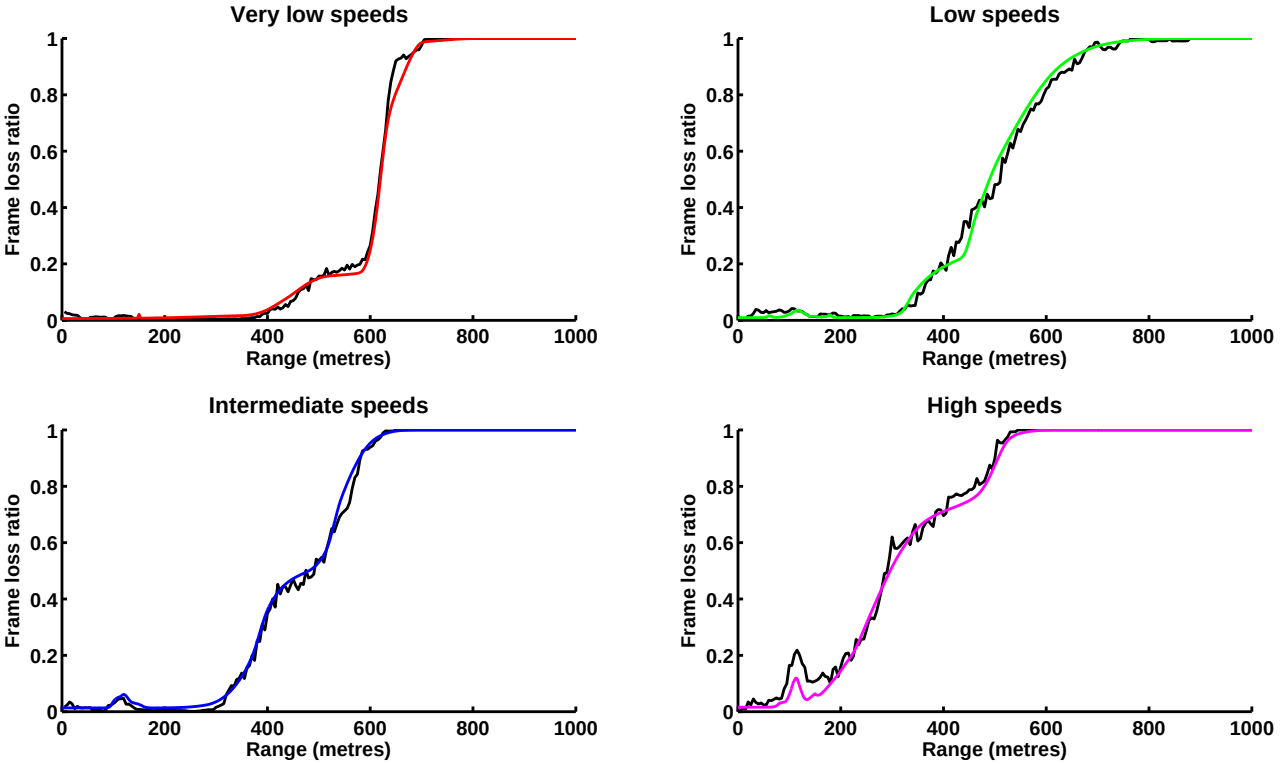

Figure 14: Averages of 1,000 profiles for each of the four classes, compared to the measured averages (in black)

model's user cannot select a specific type of influence, such as weather (the only way to do so would be to include sub-classes that would have their own distributions of $A, B, \ldots F$).

V. Conclusions and Future Works

In this paper, the results of field measurements of 802.11p are used to assess the technology's performance in actual conditions. These results are then applied to create a basic but realistic empirical model aimed at supporting high-level simulations of Cooperative Systems applications.

In terms of 802.11p performance, we have found that latency remains under 5 milliseconds in almost all circumstances, regardless of range and relative speed. We also found that frame loss remains manageable over most of the range, but that it is quite dependent on environmental conditions. Our other results are usually more pessimistic than existing literature. At the used transmission power, range showed a strong dependency on the relative speed between the emitter and the receptor. Variations apparently introduced by the direction of driving were shown to be by-products of other effects. Indeed, we have found that the vehicle's shape plays a small role in amplifying or toning down the received signal. However, the strongest effect remained with inhomogeneities in antennas, which omnidirectionality was not as good as claimed by manufacturer's data. The latter alone is sufficient to explain

effects related to the direction of driving, which vanish in more controlled conditions. The range variation depending on speed, antenna orientation and vehicle shape can amount to up to 500 metres. In better controlled conditions, the average transmission range increased and was found to be in line with the IEEE specifications for 802.11p, or even exceeding them. However, they remained subject to influence by the weather (especially, it appears, the air relative humidity).

Such range variations have important implication for Cooperative Systems, as they are likely to remain present in actual road conditions. At high speeds, such as when two vehicles are driving past on opposite sides of a non-segregated trunk road, the large reduction in effective range might reveal to be a problem for safety applications. Indeed, the effective range decreases to a point that IVC are not very advantageous compared to on-vehicle exteroceptive sensors such as LIDARs or RADARs, with average ranges less than 200 metres interval (when the relative speed is more than 170 km/h). Similarly, a vehicle driving past a RSU on a freeway would be able to maintain connectivity for only 600 metres (with the most generous estimate). Such limitations are very important for the dimensioning of on-vehicle perception systems.

In order to account for these limitations, we developed a 802.11p performance model that can be used to support the design of cooperative applications. Our model is capable of representing all the performance variations that we measured, contrary to previous models. It provides a frame loss probability based on the distance between two IVC devices and their relative speed, generating a frame loss profile that is unique to this connection.

For future work we intend on taking a further look at frame loss by using multiple actual IVC devices on vehicles and on roadside units to simulate a use case that features many emitting nodes at once. Indeed, this scenario can lead to VANET saturation; this scenario has been studied in theoretical simulation, but there is few experimental data collection pertaining to it. This will also allow to enhance our model, which currently does not account for the influence of multiple emitters at once. Overall, we aim at proposing guidelines for the design of efficient safety applications that use 802.11p, taking into account the latter's limitations. This will be achieved by developing cooperative perception systems within a simulated environment using our 802.11p model to get proper dimensioning and study their limitations.

ACKNOWLEDGEMENTS

This work is supported by the Commonwealth of Australia through the Cooperative Research Centre for Advanced Automotive Technology, as well as by the French Institute of Science and Technology for Transport, Development and Networks.

REFERENCES

[1] X. Yang, L. Liu, N. Vaidya, and F. Zhao, "A vehicle-to-vehicle communication protocol for cooperative collision warning," in *The First Annual International Conference on Mobile and Ubiquitous Systems: Networking and Services*, aug. 2004, pp. 114 – 123.

[2] M. Sepulcre and J. Gozalvez, "Dimensioning wave-based inter-vehicle communication systems for vehicular safety applications," in *3rd International Symposium on Wireless Communication Systems*, sept. 2006, pp. 312 –316.

[3] M. Torrent-Moreno, "Inter-vehicle communications: assessing information dissemination under safety constraints," in *Fourth Annual Conference on Wireless on Demand Network Systems and Services*, jan. 2007, pp. 59 –64.

[4] A. Böhm and M. Jonsson, "Handover in ieee 802.11p-based delay-sensitive vehicle-to-infrastructure communication," Halmstad University, Embedded Systems (CERES), Tech. Rep. IDE - 0924, 2009.

[5] M. Hassan, H. Vu, and T. Sakurai, "Performance analysis of the ieee 802.11 mac protocol for dsrc safety applications," *IEEE Transactions on Vehicular Technology*, vol. 60, no. 8, pp. 3882 –3896, oct. 2011.

[6] S. Sibecas, C. Corral, S. Emami, and G. Stratis, "On the suitability of 802.11a/ra for high-mobility dsrc," in *IEEE 55th Vehicular Technology Conference*, vol. 1, 2002, pp. 229 – 234 vol.1.

[7] J. Singh, N. Bambos, B. Srinivasan, and D. Clawin, "Wireless lan performance under varied stress conditions in vehicular traffic scenarios," in *IEEE 56th Vehicular Technology Conference*, vol. 2, 2002, pp. 743 – 747 vol.2.

[8] S. Ammoun and F. Nashashibi, "Design and efficiency measurement of cooperative driver assistance system based on wireless communication devices," *Tramsportation Research Part C: Emerging Technologies*, vol. 18, no. 3, pp. 408–428, 2010.

[9] A. Böhm, K. Lidström, M. Jonsson, and T. Larsson, "Evaluating calm m5-based vehicle-to-vehicle communication in various road settings through field trials," in *IEEE 35th Conference on Local Computer Networks*, oct. 2010, pp. 613–620.

[10] H. Guo, S. T. Goh, N. Foo, Q. Zhang, and W.-C. Wong, "Performance evaluation of 802.11p device for secure vehicular communication," in *7th International Wireless Communications and Mobile Computing Conference*, july 2011, pp. 1170 –1175.

[11] V. Shivaldova, G. Maier, D. Smely, N. Czink, A. Alonso, A. Winkelbauer, A. Paier, and C. F. Mecklenbreuker, "Performance evaluation of ieee 802.11p infrastructure-to-vehicle tunnel measurements." in *7th International Wireless Communications and Mobile Computing Conference*. IEEE, 2011, pp. 848–852.

[12] L. Cheng, B. Henty, F. Bai, and D. Stancil, "Doppler spread and coherence time of rural and highway vehicle-to-vehicle channels at 5.9 ghz," in *IEEE Global Telecommunications Conference*, 2008, pp. 1 –6.

[13] I. Tan, W. Tang, K. Laberteaux, and A. Bahai, "Measurement and analysis of wireless channel impairments in dsrc vehicular communications," in *IEEE International Conference on Communications*, may 2008, pp. 4882 –4888.

[14] S. Demmel, A. Lambert, D. Gruyer, A. Rakotonirainy, and E. Monacelli, "Empirical IEEE 802.11p performances evaluation on test tracks," in *IEEE Intelligent Vehicles Symposium*, 2012, pp. 837–842.

[15] D. Gruyer, S. Glaser, and B. Monnier, "SiVIC, a virtual platform for ADAS and PADAS prototyping, test and evaluation," in *FISITA World Automotive Congress*, June 2010.

[16] D. Gruyer, S. Demmel, B. D'Andrea-Novel, A. Lambert, and A. Rakotonirainy, "Simulation architecture for the design of cooperative collision warning systems," in *IEEE Intelligent Transportation Systems Conference*, 2012.

[17] G. Grau, D. Pusceddu, S. Rea, O. Brickley, M. Koubek, and D. Pesch, "Vehicle-2-vehicle communication channel evaluation using the cvis platform," in *Communication Systems Networks and Digital Signal Processing (CSNDSP), 2010 7th International Symposium on*, 2010, pp. 449–453.

[18] J. Mårtensson, A. Alam, S. Behere, M. Khan, J. Kjellberg, K.-Y. Liang, H. Pettersson, and D. Sundman, "The development of a cooperative heavy-duty vehicle for the gcdc 2011: Team scoop," *Intelligent Transportation Systems, IEEE Transactions on*, vol. 13, no. 3, pp. 1033–1049, 2012.

[19] I. C. Society, "IEEE standard for information technology - telecommunications and information exchange between systems - local and metropolitan area networks - specific requirements part 11: Wireless LAN medium access control (MAC) and physical layer (PHY) specifications amendment 6: Wireless access in vehicular environments," New York, 2010.

[20] A. A. Carter, "The status of vehicle-to-vehicle communication as a means of improving crash prevention performance," National Highway Traffic Safety Administration, U. S. Department of Transportation, Tech. Rep. 05-0264, 2005.

[21] A. Lambert, D. Gruyer, A. Busson, and H. M. Ali, "Usefulness of collision warning inter-vehicular system," *International Journal of Vehicle Safety*, vol. 5, no. 1, pp. 60–74, 2010.

[22] S. Demmel, D. Gruyer, J. Besnier, I. Ben Jemaa, S. Pechberti, and A. Rakotonirainy, "Collision warning dissemination in vehicles strings: An empirical measurement," in *IEEE Intelligent Vehicles Symposium*, june 2011, pp. 454 –459.

[23] C. Consortium, "Vehicle Safety Communications Project - Task 3 final report - Identify Intelligent Vehicle Safety Applications Enabled by DSRC," National Highway Traffic Safety Administration, U. S. Department of Transportation, Tech. Rep. DOT HS 809 859, 2005.

[24] C. Sommer and F. Dressler, "Using the right two-ray model? a measurement based evaluation of PHY models in VANETs," in *17th ACM International Conference on Mobile Computing and Networking*. Las Vegas, NV: ACM, september 2011.

[25] C. Sommer, D. Eckhoff, R. German, and F. Dressler, "A computationally inexpensive empirical model of IEEE 802.11p radio shadowing in urban environments," in *Eighth International Conference on Wireless On-Demand Network Systems and Services*, january 2011, pp. 84 –90.

[26] T. Mangel, O. Klemp, and H. Hartenstein, "A validated 5.9 ghz non-line-of-sight path-loss and fading model for inter-vehicle communication," in *11th International Conference on ITS Telecommunications*, august 2011, pp. 75 –80.

[27] J. Moré, "The Levenberg-Marquardt algorithm: Implementation and theory," in *Numerical Analysis*, ser. Lecture Notes in Mathematics, G. Watson, Ed. Springer Berlin / Heidelberg, 1978, vol. 630, pp. 105–116.